Noncoherent Multiple-Symbol Detection in Coded Ultra-wideband Communications

Yafei Tian and Chenyang Yang, *Member, IEEE*

***Abstract*—Recently, ultra-wideband (UWB) impulse radio systems based on noncoherent detection, such as transmitted reference and differential modulation systems, have drawn a lot of attention for their potential applications in low-rate and low-cost communications. In this paper, a unified approach is presented to develop and analyze a noncoherent multiple-symbol detection (MSD) algorithm for various UWB signaling formats in multipath environments. Pair-wise error probabilities of coherent and noncoherent MSD algorithms are derived and compared. The intrinsic connection between the coherent and noncoherent MSD algorithms is revealed, tradeoff curves between their performance and complexity are obtained, and optimal transmission signal design rules for noncoherent detection are provided. The bit error rates are shown through simulations to verify the analysis and to evaluate the performance of the developed algorithms in realistic environments.**

***Index Terms*—Coded modulation, multiple-symbol detection, noncoherent, pair-wise error probability (PEP), ultra-wideband (UWB).**

I. Introduction

ULTRA-WIDEBAND (UWB) systems transmit signals with their -10 dB bandwidths exceeding 500 MHz or 20% of their center frequencies. Impulse radio (IR) based UWB systems have unique feature of low duty-cycle signaling which is fundamentally different from conventional continuous-wave modulated narrow-band or wideband systems [1]–[3]. This has motivated studies for various novel signaling formats and detection algorithms in the last decade but the studies are far from sophisticated [4].

UWB systems can resolve densely scattered multipath components. This will dramatically reduce the signal fading thereby reducing the transmission power. However, the large amount of resolvable paths will complicate the implementation of coherent receivers. While low complexity coherent detection algorithms such as selective Rake and partial Rake were introduced [5], [6], it is worthwhile to study alternative noncoherent detection schemes in applications of low cost scenarios [7], [8]. Until now, most studies of noncoherent detection for UWB signals concentrate on the transmitted-reference (TR) [9]–[12] and differential modulation schemes [13], [14].

TR is a signaling format particularly designed for noncoherent detections, where the reference pulses and data-modulated pulses are transmitted in pairs. A pair of pulses form a frame, and usually several repeated frames are transmitted for each bit to reduce the peak power. The reference pulse remains unmodulated and keeps a fixed time interval with the data-modulated pulse. In the receiving end, the reference pulse can be delayed as a local template to demodulate the data using an autocorrelation receiver, since it experiences the same multipath channel with the data-modulated pulse. The original autocorrelation receiver has low complexity except the requirement for an analog delay line [10]. However, its performance will be degraded by the noisy template. Several studies have been devoted to improve the detection performance of TR systems. The reference pulses are averaged to obtain a cleaner template in [15]. Optimal and suboptimal noncoherent detection algorithms based on an average likelihood ratio test are studied in [16]. The principle of these algorithms is combining the received signals before analog correlations, which is referred to as predetection combining.

Differential modulation is another signaling format that can facilitate noncoherent detection. Unlike the TR scheme, differential modulation utilizes the previous symbol as a local reference template to demodulate the data. A multiple-symbol detection (MSD) algorithm for differential pulse amplitude modulated (PAM) UWB signals was studied in [14], where multiple analog correlators with different symbol delays are employed to obtain multiple correlation outputs for each symbol, then a followed sequence detector will use these correlation values. The system performance is significantly improved, but multiple analog delay lines with long and accurate delays are required. This algorithm demodulates each bit using consecutive multiple symbols simultaneously. Its principle can be traced back to the multiple-symbol differential detection (MSDD) [17].

Noncoherent detection for continuous-wave modulated signals in random time-varying channels was studied from the 1960s [18]–[21], where the received signals experience Gaussian fading channels. MSDD was first proposed for detecting M-ary phase-shift keying signals transmitted over an additive white Gaussian noise (AWGN) channel [17]. Then it was studied for spatial transmit and reception diversity signals [22]–[24]. In IR-UWB communications, the low-duty cycle signals experience channels with different characteristics from the narrow-band continuous-wave modulated signals. There are a lot of resolvable multipath components in each received

Manuscript received November 7, 2006; revised March 7, 2007, June 19, 2007, October 20, 2007, and January 23, 2008; accepted March 9, 2008. The associate editor coordinating the review of this paper and approving it for publication was D. Hong. This work was supported by the Teaching and Research Award Program for Outstanding Young Teachers in Higher Education Institutions of the Ministry of Education of P. R. China, "TRAPOYT." The material in this paper was presented in part at the IEEE International Conference on Communications, Seoul, Korea, May 2005.

The authors are with the School of Electronics and Information Engineering, Beihang University, Beijing, 100083, P. R. China (e-mail: {ytian, cyyang}@buaa.edu.cn).

Digital Object Identifier 10.1109/TWC.2008.060908.

symbol, and the channel coefficients subject to more complicated distributions. For PAM signals, the multipath channel provides reception diversity, thus the algorithm of MSDD can be applied. Nevertheless, pulse position modulation (PPM) is a nonlinear modulation, it must be transformed into a vector amplitude modulation before we derive the multiple-symbol detection algorithm. After this transformation, the equivalent channel can be described by a multiple-input-multiple-output model. Although the MSD for differential PAM signals has been studied, the detection for PPM signals can not be obtained by trivial extension. Moreover, as far as the authors known, there is no systematic study on noncoherent detection for various UWB signaling.

In this paper, we will first introduce a concept of codeword to represent various coded PAM and PPM signals, where TR and differential modulated signals can be included as two special cases. Then we will derive the noncoherent MSD algorithm in a unified framework. As an example, we will illustrate how to apply our algorithm for detecting TR signals.

We will derive the pair-wise error probability (PEP) and coding advantage for both the noncoherent and coherent MSD. These expressions can show the intrinsic connections between the length of block in the noncoherent MSD and the number of pilots in the coherent MSD. They can also show the impact of both the block length and code distance on the performance. Another important use of these expressions is for designing the optimal signaling formats of UWB pulse signals. We will examine the optimality of existing transmission schemes using the provided design rules.

This paper continues with Section II, in which the system and channel models are described. In Section III, the coherent and noncoherent multiple-symbol detection algorithms are derived. The PEP analysis and bit error rate (BER) simulation results are presented in Section IV and V. Finally, Section VI comprises concluding remarks.

II. System Description

The IR-UWB signal is composed of short pulses, on which amplitudes and positions can be modulated. We consider an information bit sequence, which are coded and modulated on a group of pulses, some on amplitudes and others on positions according to the mapping rule. The modulated pulses compose a signal block for transmission. We do not specify the detailed coding and mapping scheme. As a result, various signaling formats such as TR, differential modulation, and the concatenation of commonly used error control coding and pulse amplitude/position modulations can be included as special forms. The time-hopping or direct-sequence spreading is not taken into account explicitly. The spread signals may be dealt with in two manners: regarding the spreading process as a linear block coding, or detecting the signal after despreading. We will herein consider the symbol with only one pulse in it.

A. Transmitted Signal

Consider pulse position amplitude modulation (PPAM), while PAM or PPM can be obtained by only modulating the amplitude or position. The transmitted signal is expressed as,

$$s(t) = \sqrt{E_s} \sum_{n=0}^{N-1} a_n \phi(t - nT_s - d_n \delta_d), \tag{1}$$

where $\phi(t)$ is the normalized pulse with width T_p, $\int_0^{T_p} \phi^2(t) = 1$, E_s is the energy of a symbol, N is the number of symbols in a block, T_s is the symbol duration and $T_s \gg T_p$, a_n and d_n are the respective amplitude and position value of the nth symbol, δ_d is the modulation index which is assumed to be the same as T_p such that the position modulated pulses are orthogonal.

Since only binary PAM is desirable in practical UWB systems, a_n is restricted to $\{+1, -1\}$, and the position d_n can pick values from $\{0, \cdots, N_p - 1\}$. Define a codeword set $\{C^{(k)}\}$, where each codeword represents a sequence of uncoded information bits. Then a signal block involving N symbols is formed after coding and modulation. Select a codeword $C^{(u)}$ from $\{C^{(k)}\}$, the mapping relationship between the codeword and the amplitudes and positions of these symbols can be expressed as

$$C^{(u)} \rightarrow \{(a_0^{(u)}, d_0^{(u)}), \cdots, (a_{N-1}^{(u)}, d_{N-1}^{(u)})\}. \tag{2}$$

The transmitted signal of $C^{(u)}$ is,

$$s^{(u)}(t) = \sqrt{E_s} \sum_{n=0}^{N-1} a_n^{(u)} \phi(t - nT_s - d_n^{(u)} \delta_d). \tag{3}$$

For another possible codeword $C^{(v)}$, we can obtain the transmitted signal $s^{(v)}(t)$ which is assumed having M different symbols from $s^{(u)}(t)$ either in amplitudes or positions, where $M \leq N$. We refer to M as the code distance. Assume that among all the M symbols, there are M_1 symbols that are the same in positions but different in amplitudes, define these symbols as set η_1; there are other M_2 symbols that are different in positions and no matter if they are different in amplitudes, define these symbols as set η_2; and there are $N - M$ symbols left with identical amplitudes and positions, they are defined as set η_3, *i.e.*,

$$\begin{aligned} &\text{for } n \in \eta_1, \quad a_n^{(u)} = -a_n^{(v)}, d_n^{(u)} = d_n^{(v)}, \\ &\text{for } n \in \eta_2, \quad d_n^{(u)} \neq d_n^{(v)}, \\ &\text{for } n \in \eta_3, \quad a_n^{(u)} = a_n^{(v)}, d_n^{(u)} = d_n^{(v)}, \end{aligned}$$

where $M = M_1 + M_2$.

Position modulation can be regarded as a vector amplitude modulation, where the vector has N_p elements. Except the d_nth element, all other elements are zero. Thus we can define the transmitted amplitude vector as

$$\boldsymbol{a}_n = [0, \cdots, 0, a_n, 0, \cdots, 0]^T,$$

where $(\cdot)^T$ denotes the transpose of a vector. Since the value of a_n can be 1 or -1, the vector $\boldsymbol{a}_n$ actually represents PPAM signal. By writing the delayed pulse waveforms as a vector,

$$\boldsymbol{\phi}(t) = [\phi(t), \phi(t - \delta_d), \cdots, \phi(t - (N_p - 1)\delta_d)]^T,$$

we can obtain another expression of the transmitted signal as

$$s(t) = \sqrt{E_s} \sum_{n=0}^{N-1} \boldsymbol{a}_n^T \boldsymbol{\phi}(t - nT_s). \tag{4}$$

Through this modeling method, various coded and uncoded UWB signals can be studied in a unified framework. The possible transmitted signals are corresponding to codewords, and their differences can be described by the code distance. Since amplitude differences and position differences are defined separately, their impact on the performance can be observed individually.

B. UWB Channel Model

The multipath channel is assumed to be block fading, where the channel response $h(t)$ is invariant in a block duration. Assume that the maximal delay spread $\tau_{\max} < T_s - N_p\delta_d$, thus no intersymbol interference (ISI) exists. The multipath components usually arrive in clusters and their arrival times subject to Poisson distribution in UWB systems [25], [26]. However, since the sampling in the receiver front-end is usually equally spaced, the equivalent discrete-time channel model will be equally spaced.

Let the local reference pulse waveform be $\tilde{\phi}(t)$, a composite channel response can be defined as

$$h_c(t) = \phi(t) * h(t) * \tilde{\phi}(t), \tag{5}$$

where "$*$" denotes convolution. Sampling $h_c(t)$ with interval T_p, we obtain the equivalent discrete-time channel response

$$h_l = h_c(lT_p), l = 0, \cdots, L-1, \tag{6}$$

where $L = T_s/T_p$. Since the maximal multipath delay is $\tau_{\max}$, $h_l = 0$ when $l > \tau_{\max}/T_p$.

The magnitude of h_l subjects to the independent Nakagami-m distribution [27], and its polarity subjects to the uniform distribution, since the direction of the emitted pulse's electric field may be reversed by reflections [25]. Therefore, the probability density function of h_l is

$$p_{h_l}(h_l) = \begin{cases} \frac{1}{\Gamma(m_l)}\left(\frac{m_l}{\Omega_l}\right)^{m_l} h_l^{2m_l-1} e^{-m_l h_l^2/\Omega_l}, & h_l \geq 0 \\ \frac{1}{\Gamma(m_l)}\left(\frac{m_l}{\Omega_l}\right)^{m_l} (-h_l)^{2m_l-1} e^{-m_l h_l^2/\Omega_l}, & h_l < 0 \end{cases}, \tag{7}$$

where m_l and Ω_l are the fading figure and average power of the lth path, respectively.

C. Received Signal

For each modulation position $p \in \{0, \cdots, N_p - 1\}$, define a channel response vector

$$\boldsymbol{h}_p = [0, \cdots, h_0, \cdots, h_{L-1-p}]^T,$$

where there are p zero elements before h_0. Define an equivalent channel response matrix

$$\boldsymbol{H} = [\boldsymbol{h}_0, \cdots, \boldsymbol{h}_{N_p-1}],$$

where the N_p vectors correspond to the channel response of the transmitted symbol at N_p possible positions. For brevity, we denote $\boldsymbol{h}_0 = [h_0, \cdots, h_{L-1}]^T$ as $\boldsymbol{h}$ in the following. Given a channel realization $\boldsymbol{h}$, all other vectors can be obtained by shifting.

When the transmitted codeword is $C^{(u)}$, the received discrete signal can be expressed as

$$\boldsymbol{r}_n = \sqrt{E_s}\boldsymbol{H}\boldsymbol{a}_n^{(u)} + \boldsymbol{z}_n, \tag{8}$$

where $\boldsymbol{r}_n$ has L elements, which are the samples of the nth received symbol, $\boldsymbol{z}_n$ is a Gaussian noise vector with zero mean and covariance matrix $\boldsymbol{R}_z = E[\boldsymbol{z}_n\boldsymbol{z}_n^T] = \frac{N_0}{2}\boldsymbol{I}_L$, where $E[\cdot]$ stands for the mathematical expectation, $\frac{N_0}{2}$ is the two-sided power spectral density of the noise and $\boldsymbol{I}_L$ is an identity matrix with dimension L.

It is worth to note that the expression of (8) reflects the distinct features of IR-UWB signals and channels, where $\boldsymbol{H}$ is a multiple-input-multiple-output channel matrix, each column comprises a large number of resolvable multipath components, and each element subjects to the Nakagami-m distribution.

III. Noncoherent Multiple-symbol Detection

By using the received samples in all the N symbols, $\boldsymbol{r} = [\boldsymbol{r}_0^T, \cdots, \boldsymbol{r}_{N-1}^T]^T$, a codeword $\hat{C}^{(u)}$ can be selected as the transmitted codeword based on the maximum likelihood (ML) criterion. In this section, we will first derive the coherent MSD algorithm with known channel coefficients $\boldsymbol{h}$. Then the noncoherent MSD algorithm can be obtained by integrating the conditional probability of $\boldsymbol{r}$ over $\boldsymbol{h}$.

A. Coherent Multiple-symbol Detection

Since $\boldsymbol{z}_n$ is a vector of Gaussian noise, $\boldsymbol{r}$ subjects to multivariate Gaussian distribution conditioned on the transmitted codeword $C^{(k)}$ and channel coefficient vector $\boldsymbol{h}$ [24]. The conditional probability density function $p(\boldsymbol{r}|C^{(k)}, \boldsymbol{h})$ is therefore expressed in (9), which is at the top of the next page, where A is a constant independent from $C^{(k)}$ since $\|\boldsymbol{H}\boldsymbol{a}_n^{(k)}\|^2 = \|\boldsymbol{h}\|^2$ whatever $a_n^{(k)}$ and $d_n^{(k)}$ are, symbol $\|\cdot\|$ denotes the Frobenius norm, $y_l^{(k)}$ is the summation of the received samples in N symbols according to the assumed amplitudes $a_n^{(k)}$ and positions $d_n^{(k)}$,

$$y_l^{(k)} = \sum_{n=0}^{N-1} a_n^{(k)} r_{n,l+d_n^{(k)}}. \tag{10}$$

Let the conditional probability in (9) be maximal, we can obtain the ML estimate of $C^{(u)}$, *i.e.*,

$$\hat{C}_{\text{coh}}^{(u)} = \arg\max_{\{C^{(k)}\}} p(\boldsymbol{r}|C^{(k)}, \boldsymbol{h}) = \arg\max_{\{C^{(k)}\}} \sum_{l=0}^{L-1} y_l^{(k)} h_l. \tag{11}$$

This detection algorithm is referred to as the coherent MSD algorithm. It is shown from (10) that, (11) reduces to the conventional maximal ratio combining (MRC) detection when $N = 1$.

B. Noncoherent Multiple-symbol Detection

By averaging the conditional probability (9) on $\boldsymbol{h}$, we can obtain the probability of the received signal vector $\boldsymbol{r}$ only conditioned on the transmitted codeword $C^{(k)}$. Since the multipath components are independent of each other, we have $p(\boldsymbol{h}) = \prod_{l=0}^{L-1} p(h_l)$, thus

$$\begin{aligned} p(\boldsymbol{r}|C^{(k)}) &= \int_{-\infty}^{\infty} p(\boldsymbol{r}|C^{(k)}, \boldsymbol{h}) p(\boldsymbol{h}) d\boldsymbol{h} \\ &= A \cdot \prod_{l=0}^{L-1} \int_{-\infty}^{\infty} \exp\left[\frac{2}{N_0}\sqrt{E_s} y_l^{(k)} h_l\right] p(h_l) dh_l. \end{aligned} \tag{12}$$

$$p(\boldsymbol{r}|C^{(k)},\boldsymbol{h}) = (2\pi)^{-\frac{NJ}{2}}|\boldsymbol{R}_z|^{-\frac{N}{2}} \cdot \exp\left\{-\frac{1}{2}\sum_{n=0}^{N-1}\left(\boldsymbol{r}_n - \sqrt{E_s}\boldsymbol{H}\boldsymbol{a}_n^{(k)}\right)^T \boldsymbol{R}_z^{-1}\left(\boldsymbol{r}_n - \sqrt{E_s}\boldsymbol{H}\boldsymbol{a}_n^{(k)}\right)\right\}$$
$$= A \cdot \exp\left\{\frac{2}{N_0}\sum_{l=0}^{L-1}\sqrt{E_s}y_l^{(k)}h_l\right\} \tag{9}$$

Using the probability distribution function of h_l shown in (7) and following the equation 3.462.1 and 9.240 in [28], we obtain

$$\int_{-\infty}^{\infty}\exp\left\{\frac{2}{N_0}\sqrt{E_s}y_l^{(k)}h_l\right\}p(h_l)dh_l = {}_1F_1\left(m_l;\frac{1}{2};\frac{E_s\Omega_l(y_l^{(k)})^2}{{N_0}^2 m_l}\right), \tag{13}$$

where ${}_1F_1(\alpha;\gamma;z)$ is the Kummer confluent hypergeometric function [29], which is a series defined as

$${}_1F_1(\alpha,\gamma;z) = \frac{\Gamma(\gamma)}{\Gamma(\alpha)}\sum_{n=0}^{\infty}\frac{\Gamma(n+\alpha)}{\Gamma(n+\gamma)}\frac{z^n}{n!}. \tag{14}$$

Therefore,

$$p(\boldsymbol{r}|C^{(k)}) = A\cdot\prod_{l=0}^{L-1}\left\{{}_1F_1\left(m_l;\frac{1}{2};\frac{E_s\Omega_l(y_l^{(k)})^2}{{N_0}^2 m_l}\right)\right\}. \tag{15}$$

The computation of the Kummer function is rather involved, and the parameters m_l and Ω_l are hard to be obtained in practice. Thus we attempt to obtain a noncoherent detection algorithm without using any channel state information. We assume $m_l = \frac{1}{2}$ for all the l, that means the distribution of channel coefficients is specified as Gaussian. We also assume a flat power delay profile for the multipath channel, *i.e.*, Ω_l does not vary with l. Under these conditions, the Kummer function equals to the exponential function, *i.e.*, ${}_1F_1(\frac{1}{2};\frac{1}{2};z) = e^z$, and we can obtain a noncoherent MSD algorithm as

$$\hat{C}_{\text{non}}^{(u)} = \arg\max_{\{C^{(k)}\}} p(\boldsymbol{r}|C^{(k)}) = \arg\max_{\{C^{(k)}\}}\sum_{l=0}^{L-1}(y_l^{(k)})^2. \tag{16}$$

From (10) we know that $y_l^{(k)}$ is the summation of samples of different symbols according to the assumed amplitudes and positions. Although (16) seems to be similar to the envelop detection, the summation process behind it is critical for the implementation of the MSD algorithm. With the assumption of Gaussian distribution and flat power delay profile for the multipath fading channel, (16) is obtained without any approximation, and thus it is an optimal detector. When the assumption is not satisfied, we can still use (16) as a noncoherent detector, but it becomes suboptimal. The performance of (16) in realistic channel environments will be investigated through simulations.

The detection process in (16) is illustrated in Fig. 1 without considering the effect of noise. As an example, the received signal is a block of three symbols. In the detection, two codewords $C^{(u)}$ and $C^{(v)}$ are examined, in which $C^{(u)}$ is the correct assumption and $C^{(v)}$ is the wrong assumption. It can be seen from the lower part of the figure that, when the assumption is $C^{(u)}$, the samples will be added constructively and $(y_l^{(u)})^2$ will achieve a maximal value. Otherwise, they will be added destructively and be eliminated with each other. As a result, $(y_l^{(v)})^2$ will be less than $(y_l^{(u)})^2$.

This phenomenon is well understood for PAM signals. Since the samples of the same position in different symbols have identical magnitudes without regarding the effect of noise, the wrong assumptions of polarities will induce a reduction of decision statistics. For PPM signals, the wrong assumptions of positions will lead to a combination of different multipath components. Since the multipath components have random polarities, the decision statistics will also be reduced.

From (16), we can also obtain the analog implementation form of the noncoherent MSD algorithm, which is given in (17) at the top of the next page. The analog implementation requires long delay lines and accurate delay control. For detecting PPM signals, each codeword assumption demands a different group of delay lines.

When $N = 1$, the detectors of (16) and (17) are equivalent to conventional noncoherent energy detectors. When $N = 2$, they will behave like conventional differential detectors.

Channel variation and time offset are two factors that may degrade the system performance of the noncoherent MSD algorithm. If the channel varies in a block, or the accumulated time offset in a block exceeds the pulse width, the coherent summation of the signals from N symbols will turn into random summation even though the codeword assumption is correct. However, in most practical application scenarios of UWB systems, the channel can be considered as static in a block and the value of time offset is usually much shorter than the pulse width, thus the detection performance will not be influenced severely. If occasionally the channel varies too fast or the time offset is too large relative to the pulse width, we can shorten the block length N to accommodate the variations. The system performance will degrade with shorter N, but will still be superior to that of the conventional differential detector.

C. Example of Implementation

To illustrate how to use the noncoherent MSD algorithm for detecting various UWB signaling formats effectively, we take the TR signaling as an example in the following.

TR signaling can be viewed as a kind of linear block code followed by the pulse amplitude modulation, where each information bit is first mapped to a sequence of coded bits and afterward modulated on the amplitudes of pulses. In this example, we assume two frames are transmitted for an information bit, where each frame comprises a reference pulse and a data-modulated pulse. The reference pulse keeps unmodulated and the data-modulated pulse bears the information bit. When we use the noncoherent MSD algorithm shown in (16), we need to specify the block length N and construct the

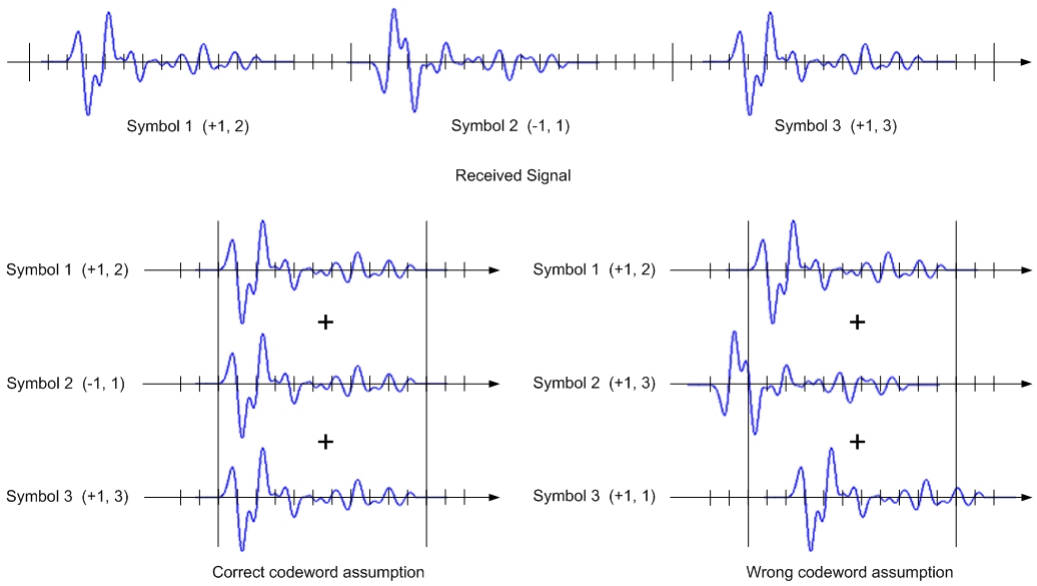

Fig. 1. Illustrating the relationship of $y_l^{(k)}$ and $C^{(k)}$ with an example, where $N = 3$, the values of a_n and d_n of the transmitted codeword are (+1,2), (-1,1) and (+1,3) in each symbol, respectively. When the codeword assumption is correct, the samples of different symbols will add constructively, otherwise, they will eliminate one another.

$$\hat{C}_{\text{non}}^{(u)} = \arg\max_{\{C^{(k)}\}} \sum_{n_1=0}^{N-1} \sum_{n_2=0}^{N-1} a_{n_1}^{(k)} a_{n_2}^{(k)} \int_0^{\tau_{\max}} r(t + n_1 T_s + d_{n_1}^{(k)} T_p) r(t + n_2 T_s + d_{n_2}^{(k)} T_p) dt. \tag{17}$$

codeword set, which decides the size of searching space and the implementation complexity.

First, we consider to use one bit duration as a block. Then the block comprises 4 pulses and N equals to 4. The information bit can be 0 or 1, which is represented by two codewords $C^{(0)}$ and $C^{(1)}$. Since only the amplitudes of pulses are modulated in TR signaling, the mapping relationship between the codewords and amplitudes of the four pulses are (see equation (2))

$$\begin{aligned} C^{(0)} &\to (1, 1, 1, 1), \\ C^{(1)} &\to (1, -1, 1, -1). \end{aligned} \tag{18}$$

The first and third elements in the parentheses are the amplitudes for reference pulses. In this simple scenario, only two codewords are included in the codeword set which need to be tested in (16). The code distance M between these two codewords is 2.

For the same TR signaling scheme, we can construct the signal block with more information bits which will improve the performance by using the noncoherent MSD. For example, we can bind the signals of the $(n-1)$th bit and the nth bit as a block. In fact, there are different ways to construct the codewords being applied in (16), which will lead to different complexity for the detectors. We can detect these two bits simultaneously each time, then there will be 4 codewords in the codeword set when using the noncoherent MSD algorithm. Another way is to sequentially detect adjacent bits and construct the signal block with one detected bit and one unknown bit. That is to say, if we have detected the $(n-1)$th bit, say it is bit 0, then the nth bit can be detected using the noncoherent MSD algorithm with only two elements in the codeword set. In this detection scheme, the previous and next signal blocks are overlapped in one bit duration. The mapping relationship for these two codewords $C^{(0)}$ and $C^{(1)}$ corresponding to bit sequences $\{0, 0\}$ and $\{0, 1\}$ are

$$\begin{aligned} C^{(0)} &\to (1, 1, 1, 1, \quad 1, 1, 1, 1), \\ C^{(1)} &\to (1, 1, 1, 1, \quad 1, -1, 1, -1). \end{aligned} \tag{19}$$

After this expansion, N increases to 8 and M is still 2. The block can be expanded even longer following this procedure.

IV. PEP Analysis

PEP is the probability that a transmitted codeword $C^{(u)}$ is incorrectly detected as a codeword $C^{(v)}$, *i.e.*, $P(C^{(u)} \to C^{(v)})$. We will derive the PEP of the coherent MSD algorithm with optimally estimated channel coefficients, as well as the PEP of the noncoherent MSD algorithm. The purpose of these derivations is not to develop a closed-form expression of the bit error rate. Instead, we aim at gaining more insight on the MSD algorithm. Through the analysis of the PEP, we will reveal the intrinsic connection between the coherent and noncoherent MSD algorithms, and provide a tradeoff curve between their performance and complexity. The optimal design rules for the transmission signal will also be provided.

A. PEP of Coherent MSD Algorithm

The coherent detection algorithm requires the knowledge of channel coefficients, which is usually obtained by channel estimation. Assume N_p pilot symbols are available and the received signal is corrupted by AWGN, then the ML estimation of channel coefficients is the average of the N_p

received symbols [30]. The estimation error e_l subjects to independent Gaussian distribution with zero mean and variance $\sigma_e^2 = \frac{N_0}{2N_pE_s}$, which is uncorrelated with the noise in the received signal of data symbols [30].

Employing (11) to detect the received signal, the pair-wise error probability is

$$P(C^{(u)} \to C^{(v)}) = P\left(\sum_{l=0}^{L-1} y_l^{(u)}\hat{h}_l < \sum_{l=0}^{L-1} y_l^{(v)}\hat{h}_l\right) = P(\Delta < 0), \tag{20}$$

where $\Delta = \sum_{l=0}^{L-1} y_l^{(u)}\hat{h}_l - \sum_{l=0}^{L-1} y_l^{(v)}\hat{h}_l$ denotes the difference between two decision statistics, $\hat{h}_l$ is the estimated channel coefficients, $\hat{h}_l = h_l + e_l$. When N_p approaches infinity, perfect channel information can be obtained, then $\hat{h}_l = h_l$. We will divide Δ into a signal part and a noise part, the signal-to-noise ratio (SNR) of Δ and PEP can then be computed.

Define $a_n = a_n^{(v)} * a_n^{(u)}$ and $d_n = d_n^{(v)} - d_n^{(u)}$. Referring to (10), $y_l^{(u)}$ can be divided into the signal component $\bar{y}_l^{(u)}$ and noise component $z_l^{(u)}$ as follows, and it is the same for $y_l^{(v)}$,

$$y_l^{(u)} = \bar{y}_l^{(u)} + z_l^{(u)}, \quad y_l^{(v)} = \bar{y}_l^{(v)} + z_l^{(v)}, \tag{21}$$

where

$$\bar{y}_l^{(u)} = \sum_{n\in\eta_1,\eta_2,\eta_3} a_n^{(u)}\sqrt{E_s}s^{(u)}_{n,l+d_n^{(u)}}, \tag{22}$$

$$\bar{y}_l^{(v)} = \sum_{n\in\eta_1,\eta_2,\eta_3} a_n^{(v)}\sqrt{E_s}s^{(u)}_{n,l+d_n^{(v)}}, \tag{23}$$

and $s_{n,l}^{(u)}$ is the lth element of $\boldsymbol{s}_n^{(u)} = \boldsymbol{H}\boldsymbol{a}_n^{(u)}$, provided that $C^{(u)}$ is the transmitted codeword. When n belongs to the symbol set η_1, we have

$$a_n^{(u)}s^{(u)}_{n,l+d_n^{(u)}} = h_l, \quad a_n^{(v)}s^{(u)}_{n,l+d_n^{(v)}} = -h_l, \tag{24}$$

when n belongs to the symbol set η_2, we have

$$a_n^{(u)}s^{(u)}_{n,l+d_n^{(u)}} = h_l, \quad a_n^{(v)}s^{(u)}_{n,l+d_n^{(v)}} = a_n h_{l+d_n}, \tag{25}$$

and when n belongs to the symbol set η_3, we have

$$a_n^{(u)}s^{(u)}_{n,l+d_n^{(u)}} = h_l, \quad a_n^{(v)}s^{(u)}_{n,l+d_n^{(v)}} = h_l. \tag{26}$$

Therefore, we can derive the signal terms in (21) as

$$\bar{y}_l^{(u)} = N\sqrt{E_s}h_l, \tag{27}$$

$$\bar{y}_l^{(v)} = (N - 2M_1 - M_2)\sqrt{E_s}h_l + \sum_{n\in\eta_2} a_n\sqrt{E_s}h_{l+d_n}. \tag{28}$$

The noise terms can be handled in a similar way, then we have

$$z_l^{(u)} = \sum_{n\in\eta_1,\eta_2,\eta_3} a_n^{(u)} z_{n,l+d_n^{(u)}} = w_{1,l} + \sum_{n\in\eta_2}\tilde{z}_{n,l} + w_{3,l}, \tag{29}$$

$$z_l^{(v)} = \sum_{n\in\eta_1,\eta_2,\eta_3} a_n^{(v)} z_{n,l+d_n^{(v)}} = -w_{1,l} + \sum_{n\in\eta_2} a_n\tilde{z}_{n,l+d_n} + w_{3,l}, \tag{30}$$

where

$$w_{1,l} = \sum_{n\in\eta_1} a_n^{(u)} z_{n,l+d_n^{(u)}}, \quad w_{3,l} = \sum_{n\in\eta_3} a_n^{(u)} z_{n,l+d_n^{(u)}}, \tag{31}$$

and $\tilde{z}_{n,l} = a_n^{(u)} z_{n,l+d_n^{(u)}}$. Since the dimension of η_1 and η_3 are M_1 and $N - M$, and $z_{n,l+d_n^{(u)}}$ is independent for different n, we can obtain the variance of $w_{1,l}$ and $w_{3,l}$ as $\frac{M_1N_0}{2}$ and $\frac{(N-M)N_0}{2}$, respectively.

Substituting the expressions of $y_l^{(u)}$ and $y_l^{(v)}$ to Δ, we have

$$\Delta = \sum_{l=0}^{L-1}(\bar{y}_l^{(u)} - \bar{y}_l^{(v)})h_l + \sum_{l=0}^{L-1}\left[(z_l^{(u)} - z_l^{(v)})h_l + (\bar{y}_l^{(u)} - \bar{y}_l^{(v)} + z_l^{(u)} - z_l^{(v)})e_l\right], \tag{32}$$

where the first term is the signal part Δ_s, and the second term is the noise part Δ_n. Since Δ_n is zero mean, the mean of Δ is still Δ_s. Through some manipulations we can obtain

$$\Delta_s = \tilde{M}\sqrt{E_s}\|\boldsymbol{h}\|^2, \tag{33}$$

where $\tilde{M} = 2M_1 + M_2$, and the variance of Δ_n is (see the Appendix)

$$\mathbb{V}\text{ar}(\Delta_n) = \tilde{M}N_0\|\boldsymbol{h}\|^2 + [\tilde{M}^2 + M_2]\frac{N_0}{2N_p}\|\boldsymbol{h}\|^2 + L\tilde{M}\frac{N_0^2}{2N_pE_s}. \tag{34}$$

Then the SNR of Δ is

$$\gamma = \frac{{\Delta_s}^2}{\mathbb{V}\text{ar}(\Delta_n)} = \frac{2\tilde{M}^2N_pE_s^2\|\boldsymbol{h}\|^4}{2\tilde{M}N_pN_0E_s\|\boldsymbol{h}\|^2 + [\tilde{M}^2 + M_2]N_0E_s\|\boldsymbol{h}\|^2 + L\tilde{M}N_0^2}. \tag{35}$$

Since the number of paths L is large, the noise part Δ_n can be approximated as Gaussian distribution [11], [15], [16]. Therefore, the PEP can be calculated as

$$P(C^{(u)} \to C^{(v)}) = Q\left(\sqrt{\gamma}\right), \tag{36}$$

where $Q(x) = 1/\sqrt{2\pi}\int_x^\infty e^{-t^2/2}dt$.

The parts of $y_l^{(u)}$ and $y_l^{(v)}$ in set η_3 are equal to each other, and they can be eliminated from Δ. Thus, no matter how large the block length N is, the PEP of the coherent MSD algorithm only depends on the dimension of η_1 and η_2, *i.e.*, M_1 and M_2.

B. PEP of Noncoherent MSD Algorithm

Employing (16) to detect the received signal, the PEP of the noncoherent MSD algorithm is

$$P(C^{(u)} \to C^{(v)}) = P\left[\sum_{l=0}^{L-1}(y_l^{(u)})^2 < \sum_{l=0}^{L-1}(y_l^{(v)})^2\right] = P(\Delta' < 0), \tag{37}$$

where $\Delta' = \sum_{l=0}^{L-1}(y_l^{(u)})^2 - \sum_{l=0}^{L-1}(y_l^{(v)})^2$.

By substituting the expressions of $y_l^{(u)}$ and $y_l^{(v)}$ provided in Section IV-A, we have

$$\Delta' = \sum_{l=0}^{L-1} \left[(\bar{y}_l^{(u)})^2 - (\bar{y}_l^{(v)})^2 \right] + \sum_{l=0}^{L-1} \left[2\bar{y}_l^{(u)} z_l^{(u)} + (z_l^{(u)})^2 - 2\bar{y}_l^{(v)} z_l^{(v)} - (z_l^{(v)})^2 \right], \quad (38)$$

where the first term is the signal part Δ'_s, and the second term is the noise part Δ'_n which also has a zero mean. Through some manipulations we have

$$\Delta'_s = [4M_1(N-M) + M_2(2N - M_2 - 1)]\, E_s \|\boldsymbol{h}\|^2, \quad (39)$$

and the variance of Δ'_n is

$$\mathbb{V}\mathrm{ar}(\Delta'_n) = N_0(2NE_s\|\boldsymbol{h}\|^2 + LN_0) \cdot [4M_1(N-M) + M_2(2N - M_2 - 1)]. \quad (40)$$

Therefore, the SNR of Δ' is

$$\gamma' = \frac{{\Delta'_s}^2}{\mathbb{V}\mathrm{ar}(\Delta'_n)} = \frac{[4M_1(N-M) + M_2(2N - M_2 - 1)]\, E_s^2 \|\boldsymbol{h}\|^4}{N_0(2NE_s\|\boldsymbol{h}\|^2 + LN_0)}. \quad (41)$$

By using the Gaussian approximation, the PEP is

$$P(C^{(u)} \to C^{(v)}) = Q\left(\sqrt{\gamma'}\right). \quad (42)$$

C. PEP Analysis

Since the Gaussian approximation is employed, the PEP only depends on the SNR of the difference of decision statistics. Therefore, we can use γ and γ' to analyze and compare the performance of coherent and noncoherent MSD algorithms.

1) Tradeoff between Performance and Complexity: First, we consider the coherent MSD algorithm. When $(\frac{N_p}{L} \cdot \frac{E_s\|\boldsymbol{h}\|^2}{N_0}) \gg 1$, we can approximate (35) as

$$\gamma \simeq \frac{\tilde{M}^2 N_p}{2\tilde{M}N_p + \tilde{M}^2 + M_2} \cdot \frac{2E_s\|\boldsymbol{h}\|^2}{N_0}, \quad (43)$$

where we define

$$G_c = \frac{\tilde{M}^2 N_p}{2\tilde{M}N_p + \tilde{M}^2 + M_2}, \quad (44)$$

as the coding advantage of the coherent MSD algorithm. It is shown that G_c does not depend on the block length N.

(35) and (36) are the conditional SNR and PEP given a channel $\boldsymbol{h}$, from which we obtained the expression of the coding advantage (44). When we derive the average PEP over $\boldsymbol{h}$, the resulted expression of the coding advantage will be the same.

Similarly, for the noncoherent MSD algorithm, when $(\frac{N}{L} \cdot \frac{E_s\|\boldsymbol{h}\|^2}{N_0}) \gg 1$, we can obtain the approximation of (41) as

$$\gamma' \simeq \frac{4M_1(N-M) + M_2(2N - M_2 - 1)}{4N} \cdot \frac{2E_s\|\boldsymbol{h}\|^2}{N_0}, \quad (45)$$

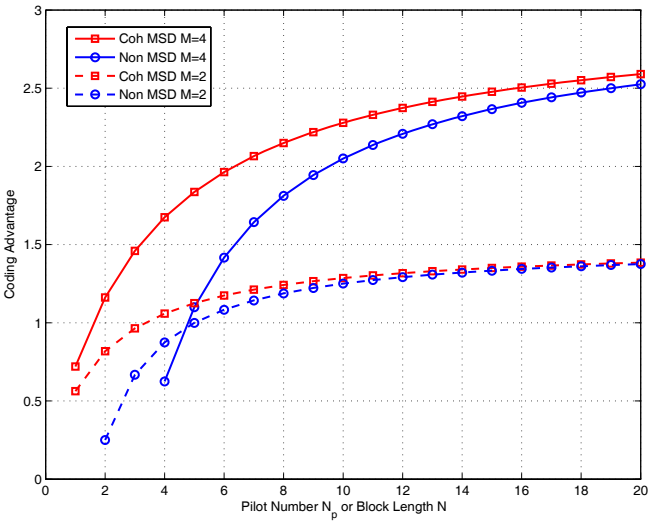

Fig. 2. The coding advantage of the coherent and noncoherent MSD algorithms, where $M_1 = M_2 = 2$ for the test cases $M = 4$, and $M_1 = M_2 = 1$ for $M = 2$.

where we define

$$G'_c = \frac{4M_1(N-M) + M_2(2N - M_2 - 1)}{4N}, \quad (46)$$

as the coding advantage of the noncoherent MSD algorithm.

The coding advantages reflect the performance gain provided by increasing the number of pilots N_p in the coherent MSD algorithm or increasing the block length N in the noncoherent MSD algorithm, when the code distance M_1 and M_2 are fixed. Figure 2 shows G_c and G'_c as functions of N_p and N, respectively, where N must be larger than the code distance M. It is shown that the coding advantages increase quickly at the initial stage, and will approach the performance limits at large N_p and N. Because the system complexity will also increase with the growing of N_p or N, these curves provide a tradeoff between the performance and complexity.

2) Connections between Coherent and Noncoherent MSDs: When N_p or N approaches infinity, the SNRs of Δ and Δ' can be derived from (35) and (41) as

$$\lim_{N_p\to\infty} \gamma = \lim_{N\to\infty} \gamma' = \frac{(2M_1 + M_2)E_s\|\boldsymbol{h}\|^2}{N_0}. \quad (47)$$

This result reveals that, the performance of the noncoherent MSD algorithm will be identical to that of the coherent MSD algorithm with perfect channel state information when the block length approaches infinity.

The coding advantages can be obtained for PAM and PPM signals separately. From (44) and (46), if only PAM is used in the transmitter, then $M_2 = 0, M = M_1$, we have

$$G_{c,\mathrm{PAM}} = \frac{MN_p}{N_p + M}, \quad G'_{c,\mathrm{PAM}} = \frac{M(N-M)}{N}. \quad (48)$$

It can be derived that $G_{c,\mathrm{PAM}} = G'_{c,\mathrm{PAM}}$ when $N_p = N - M$. This implies that $N - M$ symbols are intrinsically employed to acquire the channel state information, although there is no explicit channel estimation in the noncoherent MSD algorithm.

If only PPM is used, then $M_1 = 0, M = M_2$, we have

$$G_{c,\mathrm{PPM}} = \frac{MN_p}{2N_p + M + 1}, \quad G'_{c,\mathrm{PPM}} = \frac{M(2N - M - 1)}{4N}. \tag{49}$$

It can be shown that $G_{c,\mathrm{PPM}} = G'_{c,\mathrm{PPM}}$ when $N_p = \frac{2N-M-1}{2}$. This implies that $\frac{2N-M-1}{2}$ symbols are intrinsically used to acquire the channel state information in the noncoherent MSD algorithm for PPM signals.

3) Design Rules for the Transmitted Signal: For the coherent MSD algorithm, the performance increases monotonously with the code distance M if the block length N is given. However, this is not the case for the noncoherent MSD algorithm. From (48) and (49), we can obtain the optimal code distance M that makes the coding advantage maximal, *i.e.*,

$$\arg\max_M G'_{c,\mathrm{PAM}} = \frac{N}{2}, \quad \arg\max_M G'_{c,\mathrm{PPM}} = N - \frac{1}{2}. \tag{50}$$

Since M can not be a fraction number in practice, the optimal code distance for PPM signals should be N or $N-1$. (50) means that, while $G'_{c,\mathrm{PPM}}$ keeps increasing with M, $G'_{c,\mathrm{PAM}}$ will begin to decline when M exceeds $\frac{N}{2}$. This is because the noncoherent MSD algorithm is based on the square of the combination of the samples in N received symbols, it can not distinguish the difference of decision statistics if the polarities of the samples are all reversed. In other words, if $C^{(u)}$ and $C^{(v)}$ are totally different in polarities, *i.e.*, $M = N$ for PAM signals, their decision statistics will be the same.

Both TR signaling and differential modulation signals are PAM signals. In a sense of maximizing the coding advantage $G'_{c,\mathrm{PAM}}$, TR signaling is an optimal transmission scheme when the block length of the noncoherent MSD is restricted to one bit duration, while the differential modulation scheme is optimal when the block length in detection is restricted to two bit durations.

When PPAM is used in coded systems, some rules are required to map the coded bits to amplitudes or positions. Given the codeword distance M and block length N, the optimal configuration of M_1 and M_2 to make (46) maximal is

$$\begin{cases} M_1 = M, M_2 = 0, & \text{when } M \le N/2, \\ M_1 = N - M, M_2 = 2M - N, & \text{when } M > N/2. \end{cases} \tag{51}$$

This suggests that, when the code distance is small relative to the block length, it is better to modulate the amplitude only. When the code distance exceeds the half of the block length, it is better to modulate amplitude and position simultaneously.

V. Simulation Results

In the simulations, a Gaussian pulse with a -10 dB bandwidth of 960 MHz is transmitted, the pulse width is 2 ns. The pulse repetition time (PRT) is set to 200 ns. IEEE 802.15.4a UWB channel model [26] is employed, while the uniform phase distribution of multipath coefficients is modified to be uniform polarity distribution because of the baseband transmission. The environment 'Residential NLOS' is tested with an RMS delay spread of 19 ns, the maximal multipath delay is restricted to 200 ns, since the energy of multipath components arriving after 200 ns is negligible. A matched filter of the Gaussian pulse is placed at the receiver front-end and the sampling interval is 2 ns. The multipath coefficient vector is normalized in the channel model, $\|\boldsymbol{h}\|^2 = 1$. The SNR is defined as the ratio E_b/N_0, where E_b is the energy per information bit.

In Section IV, through PEP analysis, we obtain the relationship between the coherent and noncoherent detection, analyze the influence of adjusting the block length and code distance, *etc*. Since the BER depends on the PEP and structure of transmitted signals, the BER and PEP performance are equivalent for a given transmitted signal. This means that if a test scenario makes the PEPs of the coherent and noncoherent detection identical, their BERs will also be identical. Therefore, the previous analysis results can be verified by either PEPs or by BERs, which will not change the conclusions. In order to evaluate the performance of the developed algorithms in realistic environments, we simulate BERs, which are the averaged results over 1000 channel realizations.

The BER performance of the coherent and noncoherent MSD algorithms for the TR signaling is investigated. In the simulation, each information bit is transmitted by two pairs of reference pulses and data-modulated pulses, and is detected using the signals of multiple consecutive bits, as shown in the implementation examples in Section III-C. Therefore, there are two codewords examined in each block, and the code distance $M = 2$. Figure 3 shows the BER performance of the coherent and noncoherent MSD algorithms, where the coherent MSD is implemented with both perfect channel state information and ML channel estimation, the noncoherent MSD is implemented with various block lengths. The pilot number used for channel estimation and the block length used in the noncoherent MSD satisfy the equivalent condition obtained in Section IV-C, *i.e.*, $N_p = N - M$. Since the multipath coefficient vector is normalized, the performance of the ideal coherent detection in multipath fading channel, *i.e.*, coherent detection with perfect channel state information, is identical to that of the coherent detection in AWGN channel. It is shown that the BER of the noncoherent MSD algorithm decreases with the growing of the block length and approaches the performance of the ideal coherent detection finally. The BER curves of the coherent and noncoherent MSD algorithms are coincided exactly, which verifies our analysis. We also provide the BER of the noncoherent MSD algorithm underlying the Gaussian distributed multipath channel with flat power delay profile. This result overlays with the BER curve obtained with the 802.15.4a channel model. It implies that the detector shown in (16) performs fairly well for realistic UWB channels even though it is only optimal for the specific channels.

The ISI will be induced in the received TR signals when the PRT is shortened to be 100 and 50 ns. Figure 4 shows the BER of the coherent and noncoherent MSD algorithms in these scenarios, where the coherent MSD uses the perfect channel state information, and the noncoherent MSD detects the signal with 2 bits as a block. The ISI is moderate when PRT is 100 ns. It does not have much impact on the performance of the coherent MSD, since there is only little energy of multipath components after 100 ns. However, the performance of the noncoherent MSD algorithm becomes better than that when

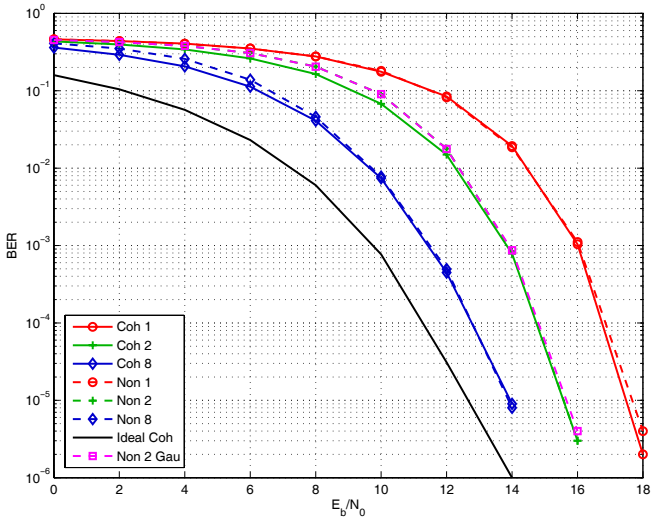

Fig. 3. The BER of a TR system, where 4 pulses are transmitted for a bit, the code distance is 2. 'Coh x' and 'Non x' are for the coherent and noncoherent MSD algorithms, respectively. The x is the number of bits involved in the noncoherent MSD, thus the block length is $4x$. Correspondingly, the pilot number used in the coherent MSD is $4x-2$. The curves for 'Coh' and 'Non' are almost coincided. 'Non 2 Gau' is for the noncoherent MSD algorithm worked in the Gaussian distributed multipath channel with flat power delay profile. The curves for 'Non 2 Gau' and 'Non 2' are overlapped.

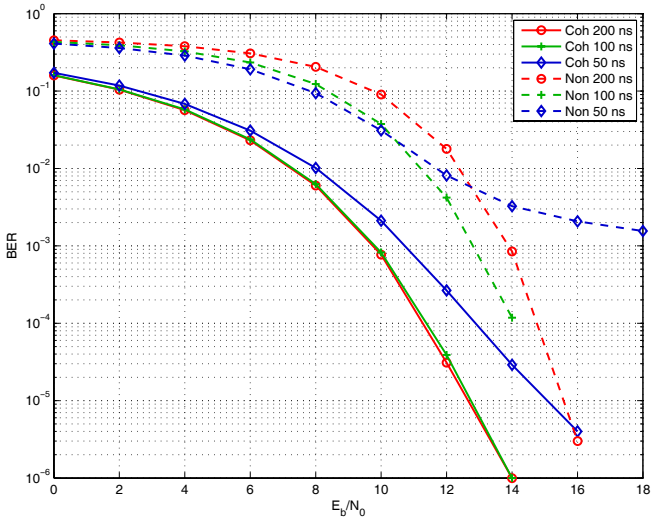

Fig. 4. The BER of three TR systems, where the PRTs are 200 ns, 100 ns and 50 ns, respectively. The ISI is induced when the PRT is less than 200 ns. The coherent MSD uses the perfect channel state information, and the noncoherent MSD detects the signal with 2 bits as a block.

PRT equals 200 ns. This is mainly because that less noise terms are combined into the sum of squares. When the PRT reduces to 50 ns, the ISI becomes severe, there is apparent performance degradation in the coherent MSD algorithm and error floor appears in the noncoherent MSD algorithm.

VI. Conclusion

In this paper, we studied the noncoherent multiple-symbol detection algorithm for general coded UWB signals, which is an important complementary scheme to the coherent detection. We introduced a unified framework for designing the noncoherent detector and analyzing its performance. Though the noncoherent MSD algorithm is only optimal for channels with Gaussian distribution and flat power delay profile, it is shown by simulations that it performs fairly well for realistic channels.

Through deriving the PEP and coding advantage, we built the inherent connection between the noncoherent and coherent MSDs, obtained the tradeoff between their performance and complexity, and provided the fundamental design rule for the transmission signals. Although the proposed algorithm is not optimal in the presence of ISI, simulation results show that it can accommodate moderate interferences.

Acknowledgment

The authors wish to thank Prof. Ye (Geoffrey) Li and Prof. Zhi Tian for their constructive discussions. We also thank the anonymous reviewers for providing a number of helpful comments.

Appendix

The variance of Δ_n, *i.e.*, equation (34) is derived below. From (32), we have

$$\Delta_n = \sum_{l=0}^{L-1} \left[(z_l^{(u)} - z_l^{(v)}) h_l + (\bar{y}_l^{(u)} - \bar{y}_l^{(v)} + z_l^{(u)} - z_l^{(v)}) e_l \right]. \tag{52}$$

Substituting (27)-(30) into (52), we get

$$\begin{aligned}\Delta_n = \sum_{l=0}^{L-1} \Bigg[& 2h_l w_{1,l} + h_l \sum_{n\in\eta_2} \tilde{z}_{n,l} - h_l \sum_{n\in\eta_2} a_n \tilde{z}_{n,l+d_n} \\ & + (2M_1 + M_2)\sqrt{E_s} h_l e_l - \sum_{n\in\eta_2} a_n \sqrt{E_s} h_{l+d_n} e_l \\ & + 2w_{1,l} e_l + \sum_{n\in\eta_2} \tilde{z}_{n,l} e_l - \sum_{n\in\eta_2} a_n \tilde{z}_{n,l+d_n} e_l \Bigg]. \end{aligned} \tag{53}$$

Reminding that $z_{n,l}$ and e_l are both independent Gaussian random variable with zero mean and variance $\sigma_z^2 = \frac{N_0}{2}$, $\sigma_e^2 = \frac{N_0}{2N_p E_s}$, and replacing $(2M_1 + M_2)$ with $\tilde{M}$, we obtain

$$\begin{aligned}\mathbb{V}\mathrm{ar}(\Delta_n) &= 4M_1\sigma_z^2 \sum_{l=0}^{L-1} h_l^2 + M_2\sigma_z^2 \sum_{l=0}^{L-1} h_l^2 + M_2\sigma_z^2 \sum_{l=0}^{L-1} h_l^2 \\ &\quad + (2M_1 + M_2)^2 E_s \sigma_e^2 \sum_{l=0}^{L-1} h_l^2 + E_s\sigma_e^2 \sum_{n\in\eta_2} \sum_{l=0}^{L-1} h_{l+d_n}^2 \\ &\quad + 4LM_1\sigma_z^2\sigma_e^2 + LM_2\sigma_z^2\sigma_e^2 + LM_2\sigma_z^2\sigma_e^2 \\ &= 2(2M_1 + M_2)\sigma_z^2 \|\boldsymbol{h}\|^2 + (2M_1 + M_2)^2 E_s\sigma_e^2 \|\boldsymbol{h}\|^2 \\ &\quad + M_2 E_s \sigma_e^2 \|\boldsymbol{h}\|^2 + 2L(2M_1 + M_2)\sigma_z^2\sigma_e^2 \\ &= \tilde{M} N_0 \|\boldsymbol{h}\|^2 + [\tilde{M}^2 + M_2] \frac{N_0}{2N_p} \|\boldsymbol{h}\|^2 + L\tilde{M} \frac{N_0^2}{2N_p E_s}. \end{aligned} \tag{54}$$

References

[1] R. A. Scholtz, "Multiple-access with time-hopping impulse modulation," in *Proc. Military Communications Conf.*, vol. 2, Boston, MA, Oct. 1993, pp. 447–450.

[2] M. Z. Win and R. A. Scholtz, "Impulse radio: how it works," *IEEE Commun. Lett.*, vol. 2, pp. 36–38, Feb. 1998.

[3] ——, "Ultra-wide bandwidth time-hopping spread-spectrum impulse radio for wireless multiple-access communications," *IEEE Trans. Commun.*, vol. 48, pp. 679–691, Apr. 2000.
[4] L. Yang and G. B. Giannakis, "Ultra-wideband communications: an idea whose time has come," *IEEE Signal Processing Mag.*, vol. 21, pp. 26–54, Nov. 2004.
[5] M. Z. Win and Z. A. Kostic, "Impact of spreading bandwidth on RAKE reception in dense multipath channels," *IEEE J. Select. Areas Commun.*, vol. 17, pp. 1794–1806, Oct. 1999.
[6] M. Z. Win, G. Chrisikos, and N. R. Sollenberger, "Performance of RAKE reception in dense multipath channels: implications of spreading bandwidth and selection diversity order," *IEEE J. Select. Areas Commun.*, vol. 18, pp. 1516–1525, Aug. 2000.
[7] R. J. Fontana, "Recent system applications of short-pulse ultra-wideband (UWB) technology," *IEEE Trans. Microwave Theory Technol.*, vol. 52, pp. 2087–2104, Sept. 2004.
[8] I. Oppermann, L. Stoica, A. Rabbachin, Z. Shelby, and J. Haapola, "UWB wireless sensor networks: UWEN–a practical example," *IEEE Commun. Mag.*, vol. 42, pp. S27–S32, Dec. 2004.
[9] C. K. Rushforth, "Transmitted-reference techniques for random or unknown channels," *IEEE Trans. Inform. Theory*, vol. 10, pp. 39–42, Jan. 1964.
[10] R. Hoctor and H. Tomlinson, "Delay-hopped transmitted-reference RF communications," in *Proc. Conf. Ultra-Wideband Syst. Technol.*, May 2002, pp. 265–270.
[11] T. Q. S. Quek and M. Z. Win, "Analysis of UWB transmitted-reference communication systems in dense multipath channels," *IEEE J. Select. Areas Commun.*, vol. 23, pp. 1863–1874, Sept. 2005.
[12] L. Yang and G. B. Giannakis, "Optimal pilot waveform assisted modulation for ultra-wideband communications," *IEEE Trans. Wireless Commun.*, vol. 3, pp. 1236–1249, July 2004.
[13] M. Ho, V. S. Somayazulu, J. Foerster, and S. Roy, "A differential detector for an ultra-wideband communications system," in *Proc. IEEE Semiann. Veh. Technol. Conf.*, May 2002, pp. 1896–1900.
[14] N. Guo and R. C. Qiu, "Improved autocorrelation demodulation receivers based on multiple-symbol detection for UWB communications," *IEEE Trans. Wireless Commun.*, vol. 5, pp. 2026–2031, Aug. 2006.
[15] J. D. Choi and W. E. Stark, "Performance of ultra-wideband communications with suboptimal receivers in multipath channels," *IEEE J. Select. Areas Commun.*, vol. 20, pp. 1754–1766, Dec. 2002.
[16] Y.-L. Chao and R. A. Scholtz, "Ultra-wideband transmitted reference systems," *IEEE Trans. Veh. Technol.*, vol. 54, pp. 1556–1569, Sept. 2005.
[17] D. Divsalar and M. K. Simon, "Multiple symbol differential detection of MPSK," *IEEE Trans. Commun.*, vol. 38, pp. 300–308, Mar. 1990.
[18] T. Kailath, "Correlation detection of signals perturbed by a random channel," *IEEE Trans. Inform. Theory*, vol. 6, pp. 361–366, June 1960.
[19] J. H. Lodge and M. L. Moher, "Maximum likelihood sequence estimation of CPM signals transmitted over Rayleigh flat-fading channels," *IEEE Trans. Commun.*, vol. 38, pp. 787–794, June 1990.
[20] W. C. Dam and D. P. Taylor, "An adaptive maximum likilihood receiver for correlated Rayleigh-fading channels," *IEEE Trans. Commun.*, vol. 42, pp. 2684–2692, Sept. 1994.
[21] X. Yu and S. Pasupathy, "Innovations-based MLSE for Rayleigh fading channels," *IEEE Trans. Commun.*, vol. 43, pp. 1534–1544, Feb./Mar./Apr. 1995.
[22] G. Caire, J. Ventura-Traveset, and E. Biglieri, "Normalized diversity receiver with multi-symbol detection," in *Proc. IEEE Global Telecommunications Conference (GLOBECOM '95)*, Nov. 1995, pp. 654–658.
[23] M. K. Simon and M.-S. Alouini, "Multiple symbol differential detection with diversity reception," *IEEE Trans. Commun.*, vol. 49, pp. 1312–1319, Aug. 2001.
[24] D. Lao and A. M. Haimovich, "Multiple-symbol differential detection with interference suppression," *IEEE Trans. Commun.*, vol. 51, pp. 208–217, Feb. 2003.
[25] J. Foerster *et al.*, "Channel modeling subcommittee final report," IEEE, Document IEEE 02490r0P802-15 SG3a, 2003.
[26] A. F. Molisch *et al.*, "IEEE 802.15.4a channel model–final report," Tech. Rep., Document IEEE 802.1504-0062-02-004a, 2005.
[27] D. Cassioli, M. Z. Win, and A. F. Molisch, "The ultra-wide bandwidth indoor channel: from statistical model to simulations," *IEEE J. Select. Areas Commun.*, vol. 20, pp. 1247–1257, Aug. 2002.
[28] I. S. Gradshteyn and I. M. Ryzhik, *Table of Integrals, Series, and Products*, 6th ed. San Diego CA: Academic Press, 2000.
[29] M. Abramowitz and I. A. Stegun, *Handbook of Mathematical Functions with Formulas, Graphs, and Mathematical Tables*, nineth ed. New York: Dover Publications, 1970.
[30] W. M. Gifford, M. Z. Win, and M. Chiani, "Diversity with practical channel estimation," *IEEE Trans. Wireless Commun.*, vol. 4, pp. 1935–1947, July 2005.

Yafei Tian received his B.S. degree in electronics engineering and Ph.D. degree in signal and information processing from Beihang University, Beijing, China, in 2001 and 2008, respectively. He is now an Assistant Professor with the School of Electronics and Information Engineering, Beihang University. His research interests lie in the areas of wireless communications and signal processing, including ultra-wideband, MIMO, and cooperative communications.

Chenyang Yang (M'98) received her M.Sc. degree in signal and information processing and Ph.D. degree in communication and information system from Beijing University of Aeronautics and Astronautics (BUAA), Beijing, China, in 1989 and 1997, respectively. She is now a Professor with the School of Electronics and Information Engineering, Beihang University (BUAA), Beijing, China. She has published various papers and holds many patents in the fields of signal processing and wireless communications. Her recent research interests include signal processing in MIMO, ultra-wideband systems, wireless sensor networks and cognitive radio.